Nonlinear Oscillations in Multibody Systems – Modeling and Stability Assessment –

W. Schiehlen

Institute B of Mechanics, University of Stuttgart
Pfaffenwaldring 9, W-7000 Stuttgart 80, Germany

Abstract. The method of multibody systems results in highly nonlinear and often high-dimensional dynamical equations featuring a broad variety of nonlinear oscillations. The generation of equations of motion, simulation tools and an approach for the stability assessment of nonlinear oscillations from an engineering point of view are presented.

1 Introduction

Mechanical systems like machines and mechanisms, spacecrafts and vehicles can be modeled properly as multibody systems for the dynamical analysis. The complexity of the dynamical equations called for the development of computer-aided formalisms a quarter of a center ago. The theoretical background is today available from a number of textbooks authored e.g. by Wittenburg [1], Ref. [2], Roberson and Schwertassek [3], Nikravesh [4], Haug [5] and Shabana [6]. The state-of-the-art is also presented at a series of IUTAM/IAVSD symposia, documented in the corresponding proceedings, see, e.g., Magnus [7], Slibar and Springer [8], Haug [9], Kortüm and Schiehlen [10], Bianchi and Schiehlen [11], Kortüm and Sharp [12].

In addition, a number of commercially distributed computer codes was developed, a summary of which is given in the Multibody Systems Handbook [13]. The computer codes available show different capabilities: some of them generate only the equations of motion in numerical or symbolical form, respectively, some of them provide numerical integration and simulation codes, too. Moreover, there are also extensive software systems on the market which offer additionally graphical data input, animation of body motions and automated signal data analysis.

The method of multibody systems is based on a finite set of elements such as rigid bodies and/or particles, bearings, joints and supports, springs and dampers, active force and/or position actuators. For the unique mathematical description of these elements a datamodel has been defined as a standardized basis for all kinds of computer codes by Otter, Hocke, Daberkow and Leister [14].

The following assumptions were agreed upon:

1. A multibody system consists of rigid bodies and ideal joints. A body may degenerate to a particle or to a body without inertia. The ideal joints include the rigid joint, the joint with completely given motion (rheonomic constraint) and the vanishing joint (free motion).

2. The topology of the multibody system is arbitrary. Chains, trees and closed loops are admitted.

3. Joints and actuators are summarized in open libraries.

4. Subsystems may be added to existing components of the multibody system.

A multibody system as defined is characterized by the class *mbs* and consists of an arbitrary number of the objects of the classes *part* and *interact*, see Figure 1.

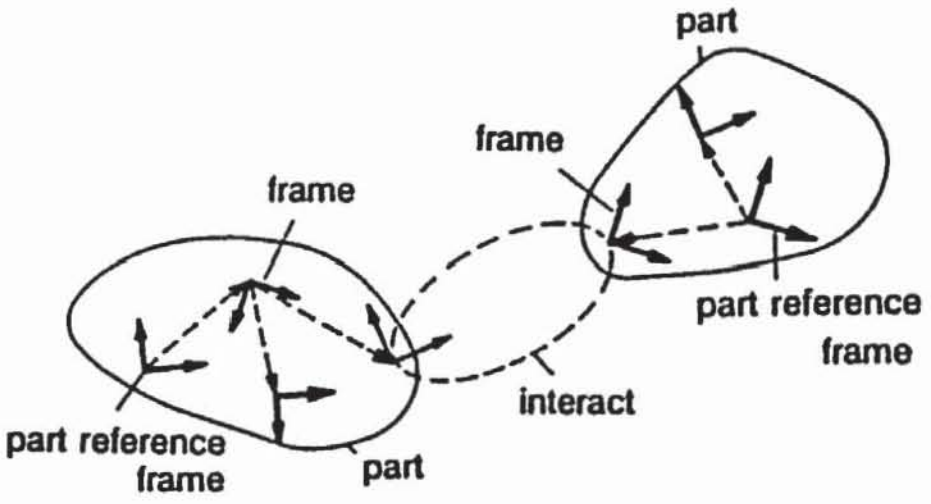

Figure 1: Multibody system to be represented by the datamodel.

The class *part* describes rigid bodies. Each *part* is characterized by at least one body-fixed *frame*, it may have a mass, a center of mass and a tensor of inertia summarized in the class *body*. The class *interact* describes the interaction between a frame on *part a* and a frame on *part b*. The interaction may be realized by a joint, by a force actuator or a sensor resulting in the classes *joint*, *force* or *sensor*, respectively. Thus, the class *interact* is characterized by two types of information: the frames to be connected and

the connecting element itself. The presented classes are the basis of the class *mbs* which means the assembled system. The model assembly using the datamodel is then easily executed. According to the definitions, the datamodel represents holonomic, rheonomic multibody systems.

2 Generation of Equations of Motion

The multibody system model has to be described mathematically by equations of motions for the dynamical analysis. The general theory for holonomic and nonholonomic systems will be presented using a minimal number of generalized coordinates for a unique representation of the motion.

2.1 Kinematics of Multibody Systems

According to the free body diagram of a mechanical system, firstly, all constraints are omitted and the system of p bodies holds $6p$ degrees of freedom. The position of the system is given relative to the inertial frame by the 3×1–translation vector

$$\mathbf{r}_i = [r_{i1}\ r_{i2}\ r_{i3}]^T \ , \quad i = 1(1)p \ , \tag{1}$$

of the center of mass C_i and the 3×3–rotation tensor

$$\mathbf{S}_i = \mathbf{S}_i(\alpha_i, \beta_i, \gamma_i) \ , \tag{2}$$

written down for each body. The rotation tensor $\mathbf{S}_i$ depends on three angles α_i, β_i, γ_i and corresponds with the direction cosine matrix relating the inertial frame I and the body-fixed frame i to each other. The $3p$ translational coordinates and the $3p$ rotational coordinates (angles) can be summarized in a $6p \times 1$–position vector

$$\mathbf{x} = [r_{11}\ r_{12}\ r_{13}\ r_{21}\ \cdots\ \alpha_p\ \beta_p\ \gamma_p]^T \ . \tag{3}$$

Eqs. (1) and (2) read now

$$\mathbf{r}_i = \mathbf{r}_i(\mathbf{x}) \ , \quad \mathbf{S}_i = \mathbf{S}_i(\mathbf{x}) \ . \tag{4}$$

Secondly, the q holonomic, rheonomic constraints are added to the mechanical system given explicitly by

$$\mathbf{x} = \mathbf{x}(\mathbf{y}, t) \,, \tag{5}$$

where the $f \times 1$ position vector

$$\mathbf{y} = [y_1 \; y_2 \; y_3 \; \cdots \; y_f]^T \tag{6}$$

is used summarizing the f generalized coordinates of the system. The number of generalized coordinates corresponds to the number of degrees of freedom, $f = 6p - q$, with respect to the system's position. Then, translation and rotation of each body follow from (4) and (5) as

$$\mathbf{r}_i = \mathbf{r}_i(\mathbf{y}, t) \,, \quad \mathbf{S}_i = \mathbf{S}_i(\mathbf{y}, t) \,. \tag{7}$$

and the velocities are found by differentiation with respect to the inertial frame:

$$\mathbf{v}_i = \dot{\mathbf{r}}_i = \frac{\partial \mathbf{r}_i}{\partial \mathbf{y}} \dot{\mathbf{y}} + \frac{\partial \mathbf{r}_i}{\partial t} = \mathbf{J}_{Ti}(\mathbf{y}, t) \dot{\mathbf{y}} + \mathbf{v}_i(\mathbf{y}, t) \,. \tag{8}$$

$$\boldsymbol{\omega}_i = \dot{\mathbf{s}}_i = \frac{\partial \mathbf{s}_i}{\partial \mathbf{y}} \dot{\mathbf{y}} + \frac{\partial \mathbf{s}_i}{\partial t} = \mathbf{J}_{Ri}(\mathbf{y}, t) \dot{\mathbf{y}} + \boldsymbol{\omega}_i(\mathbf{y}, t) \,. \tag{9}$$

The $3 \times f$ Jacobian matrices $\mathbf{J}_{Ti}$ and $\mathbf{J}_{Ri}$ defined by (8) and (9) characterize the virtual translational and rotational displacement of the system, respectively. They are also needed later for the application of d'Alembert's principle. The infinitesimal 3×1 rotation vector $\mathbf{s}_i$ used in (9) follows analytically from the corresponding infinitesimal skew symmetrical 3×3 rotation tensor. However, the matrix $\mathbf{J}_{Ri}$ can also be found by a geometrical analysis of the angular velocity vector $\boldsymbol{\omega}_i$ with respect to the angles α_i, β_i, γ_i, see e.g. Ref. [2].

The accelerations are obtained by a second differentiation with respect to the inertial frame:

$$\mathbf{a}_i = \mathbf{J}_{Ti}(\mathbf{y}, t) \ddot{\mathbf{y}} + \frac{\partial \mathbf{v}_i}{\partial \mathbf{y}} \dot{\mathbf{y}} + \frac{\partial \mathbf{v}_i}{\partial t} \,, \tag{10}$$

$$\boldsymbol{\alpha}_i = \mathbf{J}_{Ri}(\mathbf{y}, t) \ddot{\mathbf{y}} + \frac{\partial \boldsymbol{\omega}_i}{\partial \mathbf{y}} \dot{\mathbf{y}} + \frac{\partial \boldsymbol{\omega}_i}{\partial t} \,. \tag{11}$$

For scleronomic constraints the partial time–derivatives in (8), (9) and (10), (11) vanish.

Thirdly, the r nonholonomic, rheonomic constraints, especially due to rigid wheels, are introduced explicitly by

$$\dot{\mathbf{y}} = \dot{\mathbf{y}}(\mathbf{y}, \mathbf{z}, t) \tag{12}$$

with the $g \times 1$–velocity vector

$$\mathbf{z}(t) = [z_1 \; z_2 \; z_3 \; \cdots \; z_g]^T \tag{13}$$

summarizing the g generalized velocities of the system. The number of generalized velocities characterizes the number of degrees of freedom, $g = f - r$, with respect to the system's velocity. From (8), (9) and (12) the translational and rotational velocity of each body follow immediately as

$$\mathbf{v}_i = \mathbf{v}_i(\mathbf{y}, \mathbf{z}, t) \; , \quad \boldsymbol{\omega}_i = \boldsymbol{\omega}_i(\mathbf{y}, \mathbf{z}, t) \; . \tag{14}$$

The accelerations are found again by differentiation with respect to inertial frame I:

$$\mathbf{a}_i = \frac{\partial \mathbf{v}_i}{\partial \mathbf{z}} \dot{\mathbf{z}} + \frac{\partial \mathbf{v}_i}{\partial \mathbf{y}} \dot{\mathbf{y}} + \frac{\partial \mathbf{v}_i}{\partial t} = \mathbf{L}_{Ti}(\mathbf{y}, \mathbf{z}, t)\, \dot{\mathbf{z}} + \dot{\bar{\mathbf{v}}}_i(\mathbf{y}, \mathbf{z}, t) \; , \tag{15}$$

$$\boldsymbol{\alpha}_i = \frac{\partial \boldsymbol{\omega}_i}{\partial \mathbf{z}} \dot{\mathbf{z}} + \frac{\partial \boldsymbol{\omega}_i}{\partial \mathbf{y}} \dot{\mathbf{y}} + \frac{\partial \boldsymbol{\omega}_i}{\partial t} = \mathbf{L}_{Ri}(\mathbf{y}, \mathbf{z}, t)\, \dot{\mathbf{z}} + \dot{\bar{\boldsymbol{\omega}}}_i(\mathbf{y}, \mathbf{z}, t) \; . \tag{16}$$

Here, the $3 \times g$ matrices $\mathbf{L}_{Ti}$ and $\mathbf{L}_{Ri}$ describe the virtual translational and rotational velocity of the system needed also for the application of Jourdain's principle. Further, it has to be mentioned that the partial time–derivatives vanish in (15), (16) for scleronomic systems.

2.2 Newton–Euler Equations

For the application of Newton's and Euler's equations to multibody systems the free body diagram has to be used again. Now the rigid bearings and supports are replaced by adequate constraint forces and torques as discussed later in this section.

Newton's and Euler's equations read for each body in the inertial frame

$$m_i \dot{\mathbf{v}}_i = \mathbf{f}_i^e + \mathbf{f}_i^r \,, \quad i = 1(1)p \,, \tag{17}$$

$$\mathbf{I}_i \dot{\boldsymbol{\omega}}_i + \tilde{\boldsymbol{\omega}}_i \mathbf{I}_i \boldsymbol{\omega}_i = \mathbf{l}_i^e + \mathbf{l}_i^r \,, \quad i = 1(1)p \,. \tag{18}$$

The inertia is represented by the mass m_i and the 3×3 inertia tensor $\mathbf{I}_i$ with respect to the center of mass C_i of each body. The external forces and torques in (17) and (18) are composed by the 3×1 applied force vector $\mathbf{f}_i^e$ and torque vector $\mathbf{l}_i^e$ due to springs, dampers, actuators, weight etc. and by the 3×1 constraint force vector $\mathbf{f}_i^r$ and torque vector $\mathbf{l}_i^r$. All torques are related to the center of mass C_i. The applied forces and torques, respectively, depend on the motion by different laws and they may be coupled to the constraint forces and torques in the case of friction.

The constraint forces and torques originate from the reactions in joints, bearings, supports or wheels. They can be reduced by distribution matrices to the generalized constraint forces. The number of the generalized constraint forces is equal to the total number of constraints $(q + r)$ in the system. Introducing the $(q + r) \times 1$ vector of generalized constraint forces

$$\mathbf{g} = [g_1 \; g_2 \; g_3 \; \cdots \; g_{q+r}]^t \tag{19}$$

and the $3 \times (q + r)$ distribution matrices

$$\mathbf{F}_i = \mathbf{F}_i(\mathbf{y}, \mathbf{z}, t) \,, \quad \mathbf{L}_i = \mathbf{L}_i(\mathbf{y}, \mathbf{z}, t) \tag{20}$$

it turns out

$$\mathbf{f}_i^r = \mathbf{F}_i \mathbf{g} \,, \quad \mathbf{l}_i^r = \mathbf{L}_i \mathbf{g} \,, \quad i = 1(1)p \,, \tag{21}$$

for each body. The constraint forces or the distribution matrices, respectively, can be found analytically or they are derived by geometrical analysis.

The ideal applied forces and torques depend only on the kinematical variables of the system, they are independent of the constraint forces. Ideal applied forces are due to the elements of multibody systems, and further actions on the system, e.g. gravity. The forces may be characterized by proportional, differential and/or integral behavior.

The proportional forces are characterized by the system's position and timefunctions

$$\mathbf{f}_i^e = \mathbf{f}_i^e(\mathbf{x}, t) \,. \tag{22}$$

E.g., conservative spring and weight forces as well as purely time-varying forces are proportional forces.

The proportional differential forces depend on the position and the velocity:

$$\mathbf{f}_i^r = \mathbf{f}_i^r(\mathbf{x}, \dot{\mathbf{x}}, t) \ . \tag{23}$$

A parallel spring dashpot configuration is a typical example for this kind of forces. The proportional integral forces are a function of the position and integrals of the position:

$$\mathbf{f}_i^r = \mathbf{f}_i^r(\mathbf{x}, \mathbf{w}, t) \ , \quad \dot{\mathbf{w}} = \dot{\mathbf{w}}(\mathbf{x}, \mathbf{w}, t) \ . \tag{24}$$

where the $p \times 1$-vector $\mathbf{w}$ describes the position integrals. E.g., serial spring-damper configurations and the eigendynamics of actuators result in proportional-integral forces. In vehicle systems proportional-integral forces appear, e.g., with modern engine mounts for simultaneous noise and vibration reduction. The same laws hold also for ideal applied torques.

In the case of nonideal constraints with sliding friction or contact forces, respectively, the applied forces are coupled with the constraint forces.

The Newton Euler equations of the complete system are summarized in matrix notation by the following vectors and matrices. The inertia properties are written in the $6p \times 6p$ diagonal matrix

$$\mathbf{M} = diag\{m_1 \mathbf{E} \ m_2 \mathbf{E} \ \cdots \ \mathbf{I}_1 \ \cdots \ \mathbf{I}_p\} \ , \tag{25}$$

where the 3×3 identity matrix $\mathbf{E}$ is used. The $6p \times 1$ force vectors $\mathbf{q}^c$, $\mathbf{q}^e$, $\mathbf{q}^r$ representing the coriolis forces, the ideal applied forces and the constraint forces, respectively, are given by the following scheme,

$$\mathbf{q} = \left[\mathbf{f}_1^T \ \mathbf{f}_2^T \ \cdots \ \mathbf{I}_1^T \ \cdots \ \mathbf{I}_p^T\right]^T \ . \tag{26}$$

Further the $6p \times f$-matrix $\mathbf{J}$ and $6p \times g$-matrix $\bar{\mathbf{L}}$ as well as the $6p \times (q+r)$-distribution matrix $\bar{\mathbf{Q}}$ are introduced as global matrices, e.g.,

$$\mathbf{J} = \left[\mathbf{J}_{T1}^T \ \mathbf{J}_{T2}^T \ \cdots \ \mathbf{J}_{R1}^T \ \cdots \mathbf{J}_{Rp}^T\right]^T \ . \tag{27}$$

Now, the Newton-Euler equations can be represented as follows for holonomic systems in the inertial frame

$$\mathbf{M}\,\mathbf{J}\,\dot{\mathbf{y}} + \mathbf{q}^c(\mathbf{y}, \dot{\mathbf{y}}, t) = \mathbf{q}^e(\mathbf{y}, \dot{\mathbf{y}}, t) + \mathbf{Q}\,\mathbf{g} \tag{28}$$

and for nonholonomic systems

$$\mathbf{M}\,\mathbf{L}\,\dot{\mathbf{z}} + \mathbf{q}^c(\mathbf{y}, \mathbf{z}, t) = \mathbf{q}^e(\mathbf{y}, \mathbf{z}, t) + \mathbf{Q}\,\mathbf{g} \tag{29}$$

If the holonomic constraints are omitted, e.g. $\mathbf{z} = \dot{\mathbf{y}}$, eq.(29) reduces to (28), showing a close relation between both representations.

2.3 Equations of Motion

The Newton-Euler equations are combined algebraical and differential equations and the question arises if they can be separated for solution into purely algebraical and differential equations. There is a positive answer given by the dynamical principles. In a first step, the system's motion can be found by integration of the separated differential equations and in a second step the constraint forces are calculated algebraically. For ideal applied forces both steps can be executed successively while contact forces require simultaneous execution.

Holonomic systems with proportional or proportional differential forces result in *ordinary* multibody systems. The equations of motion follow from the Newton-Euler equations, applying d'Alembert's principle.

The equations of motion of holonomic systems are found according to d'Alembert's principle by premultiplication of (28) with $\mathbf{J}^T$ as

$$\mathbf{M}(\mathbf{y}, t)\,\ddot{\mathbf{y}} + \mathbf{k}(\mathbf{y}, \dot{\mathbf{y}}, t) = \mathbf{q}(\mathbf{y}, \dot{\mathbf{y}}, t)\,. \tag{30}$$

Here, the number of equations is reduced from $6p$ to f, the $f \times f$ inertia matrix $\mathbf{M}(\mathbf{y}, t)$ is completely symmetrized $\mathbf{M}(\mathbf{y}, t) = \mathbf{J}^T\mathbf{M}\mathbf{J} > 0$, and the constraint forces and torques are eliminated. The remaining $f \times 1$ vector $\mathbf{k}$ describes the generalized coriolis forces and the $f \times 1$ vector $\mathbf{q}$ includes the generalized applied forces.

Nonholonomic systems with proportional integral forces produce *general* multibody systems. The equations of motion are obtained from the Newton-Euler equations (29) where the proportional integral forces (24) and Jourdain's principle has to be regarded. However, the equations of motion are not sufficient, they have to be completed by the nonholonomic constraint equation (12). Thus, the complete equations read as

$$\begin{aligned} &\mathbf{M}(\mathbf{y},\mathbf{z},t)\,\dot{\mathbf{z}} + \mathbf{k}(\mathbf{y},\mathbf{z},t) = \mathbf{q}(\mathbf{y},\mathbf{z},\mathbf{w},t)\ , \\ &\dot{\mathbf{y}} = \dot{\mathbf{y}}(\mathbf{y},\mathbf{z},t)\ , \quad \dot{\mathbf{w}} = \dot{\mathbf{w}}(\mathbf{y},\mathbf{z},t)\ . \end{aligned} \tag{31}$$

Now, the number of equations is reduced from $6p$ to g and the $g \times g$-symmetric inertia matrix $\mathbf{M}(\mathbf{y},t) = \bar{\mathbf{L}}^T\mathbf{M}\bar{\mathbf{L}} > 0$ appears. Further, $\mathbf{k}$ and $\mathbf{q}$ are $g \times 1$-vectors of generalized coriolis and applied forces. The equations (31) are in the literature also denoted as Kane's equations.

In addition to the mechanical representation (31) of a multibody system, there exists also the possibility to use the more general representation of dynamical systems in the state space, i.e.,

$$\dot{\mathbf{x}} = \mathbf{f}(\mathbf{x},t)\ , \tag{32}$$

where $\mathbf{x}$ means the $n \times 1$ state vector composed of generalized coordinates and velocities, and t the time, respectively.

The constraint forces are completely omitted by the dynamical principles. However, they are also of engineering interest for the load in joints, bearings and supports, and they are absolutely necessary for the computation of contact and friction forces. From the $6p$ coordinates of the constraint force vector $\bar{\mathbf{q}}^r$ there are only $(q+r)$ coordinates linear independent according to (21). Therefore, only the $(q+r) \times 1$-vector $\mathbf{g}$ of the generalized constraint forces is needed. The results are given for holonomic systems only, $r = 0$, but they can be transferred to nonholonomic systems without any problem.

Premultiplication of (28) by $\mathbf{Q}^T\mathbf{M}^{-1}$ results according to d'Alembert's principle immediately in the equations of reaction

$$\mathbf{N}(\mathbf{y},t)\,\mathbf{g} + \hat{\mathbf{q}}(\mathbf{y},\dot{\mathbf{y}},t) = \hat{\mathbf{k}}(\mathbf{y},\dot{\mathbf{y}},t) \tag{33}$$

where $\mathbf{N}(\mathbf{y},t)$ is the symmetrical $q \times q$-reaction matrix and $\hat{\mathbf{q}}$ and $\hat{\mathbf{k}}$ are $q \times 1$-vectors.

2.4 Formalism NEWEUL

The equations of motion presented may be automatically generated by the formalism NEWEUL described in the Multibody Systems Handbook [13], too.

NEWEUL is a software package for the dynamic analysis of mechanical systems with the multibody system method. It comprises the computation of the symbolic equations of motion.

NEWEUL has been successfully applied in industrial and academic research institutions since 1979. The major fields of application are vehicle dynamics, dynamics of machinery, robot dynamics, biomechanics, satellite dynamics, and dynamics of mechanisms. The input data for NEWEUL have to be entered in input files prepared with prompts and comments.

The resulting equations of motion may be linear, partially linearized, or nonlinear symbolic differential equations. Constant parameters can be included in numerical form. Nonlinear coupling elements in kinematically linear models are also permitted.

For the output format of the equations of motion several options are possible. A FORTRAN compatible output allows the equations to be included in commercial software packages for dynamic analysis and simulation such as, for instance, ACSL. Another output format allows the processing of the equations with the formula manipulation program MAPLE.

The software module NEWSIM included in the NEWEUL package allows the simulation of motion by numerical integration of the symbolic equations of motion provided. It automatically generates a problem specific simulation program. The user simply has to add the specification of force laws, system parameter values, and initial conditions. The simulation results are stored in ASCII data files that can be visualized with arbitrary graphics packages.

The simulation results may contain the time history of the state variables, the kinematical data of observation points, data for animation, the time history of the reaction forces, and user defined output data.

The software package NEWEUL is written in FORTRAN 77 and can be implemented on any workstation or mainframe with a FORTRAN 77 compiler. NEWEUL uses its own formula manipulator.

3 Stability Assessment

The dynamical equations of multibody systems describing autonomous nonlinear oscillations are represented in a canonical form as

$$\dot{\mathbf{x}} = \mathbf{f}(\mathbf{x}), \qquad \mathbf{x}(t_0) = \mathbf{x}_0 \tag{34}$$

following from (32). Here is $\mathbf{x}$ the $n \times 1$ state vector, $\mathbf{f}$ an $n \times 1$ vector function and t means the time. At initial time t_0 the initial state $\mathbf{x}_0$ is given. It is assumed that $\mathbf{f}(\mathbf{0}, t) = \mathbf{0}$ represents an equilibrium position $\mathbf{x} = \mathbf{0}$. Due to the nonlinearity of the system, there may exist additional equilibrium positions $\mathbf{x} = \mathbf{x}^*$.

3.1 Stability definition

The stability in the sense of Ljapunov characterizes the qualitative behaviour of the equilibrium position $\mathbf{x} = \mathbf{0}$ of the dynamical system (34). For the stability definition the absolute value norm of a vector is used.

The time variant norm of the $n \times 1$ -state vector

$$\mathbf{x}(t) = [x_1(t) \ \cdots \ x_n(t)]^T \ , \quad t \in [t_0, \infty) \tag{35}$$

is defined as

$$\|\mathbf{x}(t)\| := \max_{1 \le i \le n} |x_i(t)| \ . \tag{36}$$

The time interval norm reads as

$$\|\mathbf{x}(t)\|_T := \max_{t \in [t_0, T]} \|\mathbf{x}(t)\| \tag{37}$$

where time T may approach infinity,

$$\|\mathbf{x}(t)\|_\infty := \lim_{T \to \infty} \|\mathbf{x}(t)\|_T \ . \tag{38}$$

These definitions are also valid for matrices, e.g.,

$$\|\mathbf{A}\| := \max_{1 \le i \le n} \sum_{j=1}^{n} |a_{ij}| \ . \tag{39}$$

The dynamical system (34) is called stable (in the sense of Ljapunov) if for every positive $\varepsilon > 0$ there exists a positive number $\delta = \delta(\varepsilon) > 0$ such that for all initial conditions bounded by

$$||\mathbf{x}_0|| < \delta = \delta(\varepsilon) \tag{40}$$

the corresponding trajectories $\mathbf{x}(t)$ remain bounded for all t:

$$||\mathbf{x}(t)|| < \varepsilon \ . \tag{41}$$

The dynamical system (34) is asymptotically stable if it is stable and for all bounded initial conditions (40) the corresponding trajectory tends to zero

$$\lim_{t\to\infty} ||\mathbf{x}(t)|| = 0 \,. \tag{42}$$

If the dynamical system (34) is not stable it will be called unstable.

Based on these definitions, there exists a large literature on stability problems, and quite a number of textbooks, e.g., Hahn [15] and P.C. Müller [16]. However, the stability analysis provides only a qualitative answer. For engineering applications some quantitative global information on the dynamical behaviour is of interest. This can be obtained by a stability assessment.

3.2 Stability assessment

Based on the stability definitions in the sense of Ljapunov the following stability measures are defined.

The stability measure $S1$ or its inverse $IS1$, respectively,

$$IS1(\mathbf{x}_0, t_0) = \frac{1}{S1(\mathbf{x}_0, t_0)} = \begin{cases} \dfrac{\|\mathbf{x}(t)\|_\infty}{\|\mathbf{x}_0\|} & \text{for } \mathbf{x}_0 \neq \mathbf{0} \\ 1 & \text{for } \mathbf{x}_0 = \mathbf{0} \end{cases} \tag{43}$$

characterizes the ratio between a given initial state $\mathbf{x}_0$ and the corresponding maximal displacement of the trajectory. The measure $S1$ depends on $\mathbf{x}_0$ and t_0.

The inverse stability measure

$$IS2(r, t_0) := \max_{\mathbf{x}_0 \in \{\mathbf{x}\,|\,\|\mathbf{x}\|=r\}} IS1(\mathbf{x}_0, t_0) \tag{44}$$

is defined for a subspace of the initial conditions' state space. The inverse measure $IS2$ characterizes the maximal displacement of all trajectories starting out of the initial conditions' subspace which is by definition a hyper-cube with respect to the equilibrium point $\mathbf{x} = \mathbf{0}$. By definition it yields

$$IS1 \geq 1 \,, \quad IS2 \geq 1 \,. \tag{45}$$

In a numerical analysis the integration interval is limited. Then, the measures (43) and (44) have to be replaced by

$$IS1_T(\mathbf{x}_0, t_0) := \frac{\|\mathbf{x}(t)\|_T}{\|\mathbf{x}_0\|} , \tag{46}$$

$$IS2_T(r, t_0) := \max_{\mathbf{x}_0 \in \{\mathbf{x}, \|\mathbf{x}\| = r\}} S1_T(\mathbf{x}_0, t_0) . \tag{47}$$

For autonomous systems

$$\dot{\mathbf{x}} = \mathbf{f}(\mathbf{x}) , \quad \mathbf{x}(t_0) = \mathbf{x}_0 \tag{48}$$

the initial time can be chosen as $t_0 = 0$ without any restriction to the generality.

There is a direct relation between the stability and the above defined stability measures. For an instable system one may choose a series of initial conditions satisfying $\|\mathbf{x}_{0_1}\| > \|\mathbf{x}_{0_2}\| > \cdots > \|\mathbf{x}_{0_n}\|$. Then it yields

$$\lim_{n \to \infty} \|\mathbf{x}_{0_n}\| = 0 \quad \text{and} \quad \lim_{n \to \infty} IS1(\mathbf{x}_{0_n}, t_0) = \infty . \tag{49}$$

On the other hand, if the inverse stability measure $IS1$ is limited, then

$$\|\mathbf{x}(t)\|_\infty \leq s \|\mathbf{x}_0\| . \tag{50}$$

This means $\|\mathbf{x}(t)\|_\infty \to 0$ for $\|\mathbf{x}_0\| \to 0$, i.e., the system is stable in the sense of Ljapunov.

Usually the components of the state vector, $x_1(t), \cdots, x_n(t)$, have different units. For the application of the stability measures it is necessary that all components have the same unit. This can be achieved by standardizing operations.

The stability measures defined characterize dynamical systems of arbitrary dimension by a scalar number. Therefore, they are especially well suited for the multibody system analysis. More sophisticated geometric measures of analysis are usually restricted to two or at most three dimensions.

The above defined stability measures may be applied to linear systems, too, see Hu [17].

3.3 The single pendulum

The single pendulum will be used as a first example, since, in addition to the numerical solution, an analytical solution is available. The equation of motion reads without units as

$$\varphi'' + \sin\varphi = 0 \ . \tag{51}$$

After some calculation, the following results are obtained,

for $\varphi_0'^2 \leq 2(1+\cos\varphi_0)$

$$IS1(\mathbf{x}_0) = \frac{\max\{\sqrt{\varphi_0'^2 + 2(1-\cos\varphi_0)}\ , \arccos(\cos\varphi_0 - \varphi_0'^2/2)\}}{\max(|\varphi_0|, |\varphi_0'|)} \ , \tag{52}$$

for $\varphi_0'^2 > 2(1+\cos\varphi_0)$

$$IS1(\mathbf{x}_0) = \infty \ , \tag{53}$$

and for $0 < r \leq r^*$

$$IS2(r) = \frac{\arccos(\cos r - r^2/2)}{r} \ , \tag{54}$$

for $r > r^*$

$$IS2(r) = \infty \ , \tag{55}$$

where $r^* = 1.478$ follows as a root of the equation $r^2 = 2(1+\cos r)$. Figure 2 presenting the stability measure $IS2$ shows clearly the instability of the equilibrium position $\mathbf{x} = \mathbf{0}$ for a sufficiently large initial angular velocity.

The corresponding phase portrait, Figure 3, shows three rectangles of initial conditions, namely $r = 0.5;\ 1.0;\ 1.478$. Using numerical results of a time interval $T = 100$, the stabilty measure $IS1_T$ can be visualized, too, Figure 4. It is observed that initial conditions of the second component of the state vector, $x_2 = \varphi'$, i.e., the initial velocities, are more critical than initial displacements.

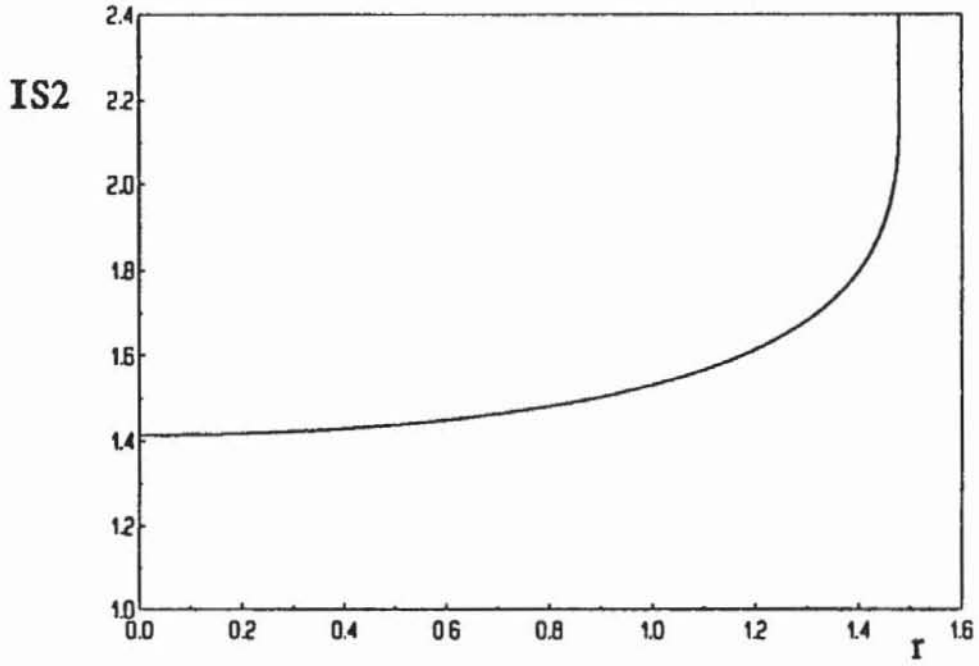

Figure 2: Stability measure $IS2$ of the single pendulum.

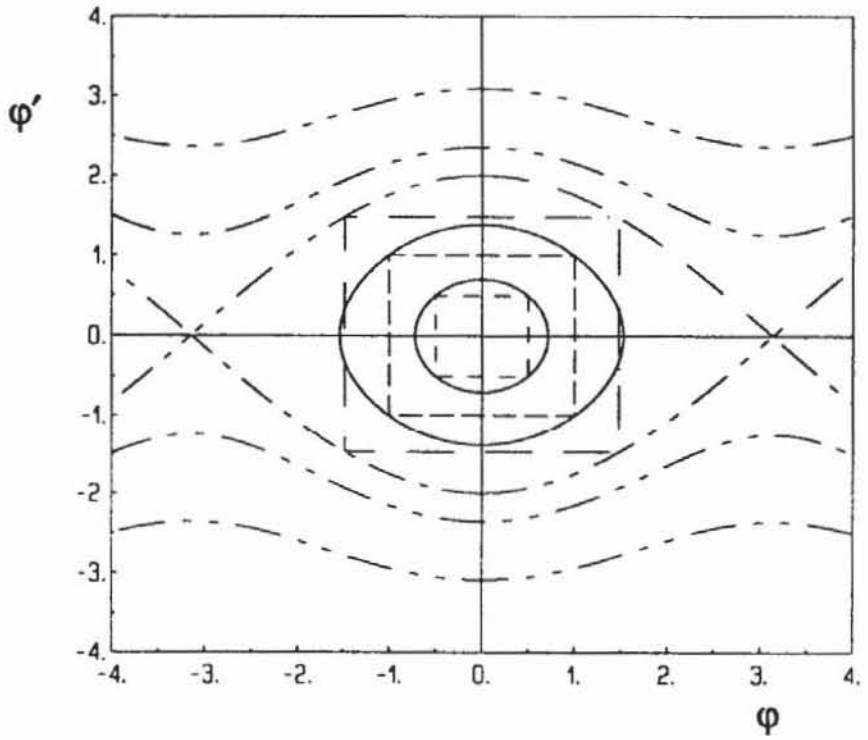

Figure 3: Phase portrait of the single pendulum with three rectangles of initial conditions $r = 0.5;\ 1.0;\ 1.478$.

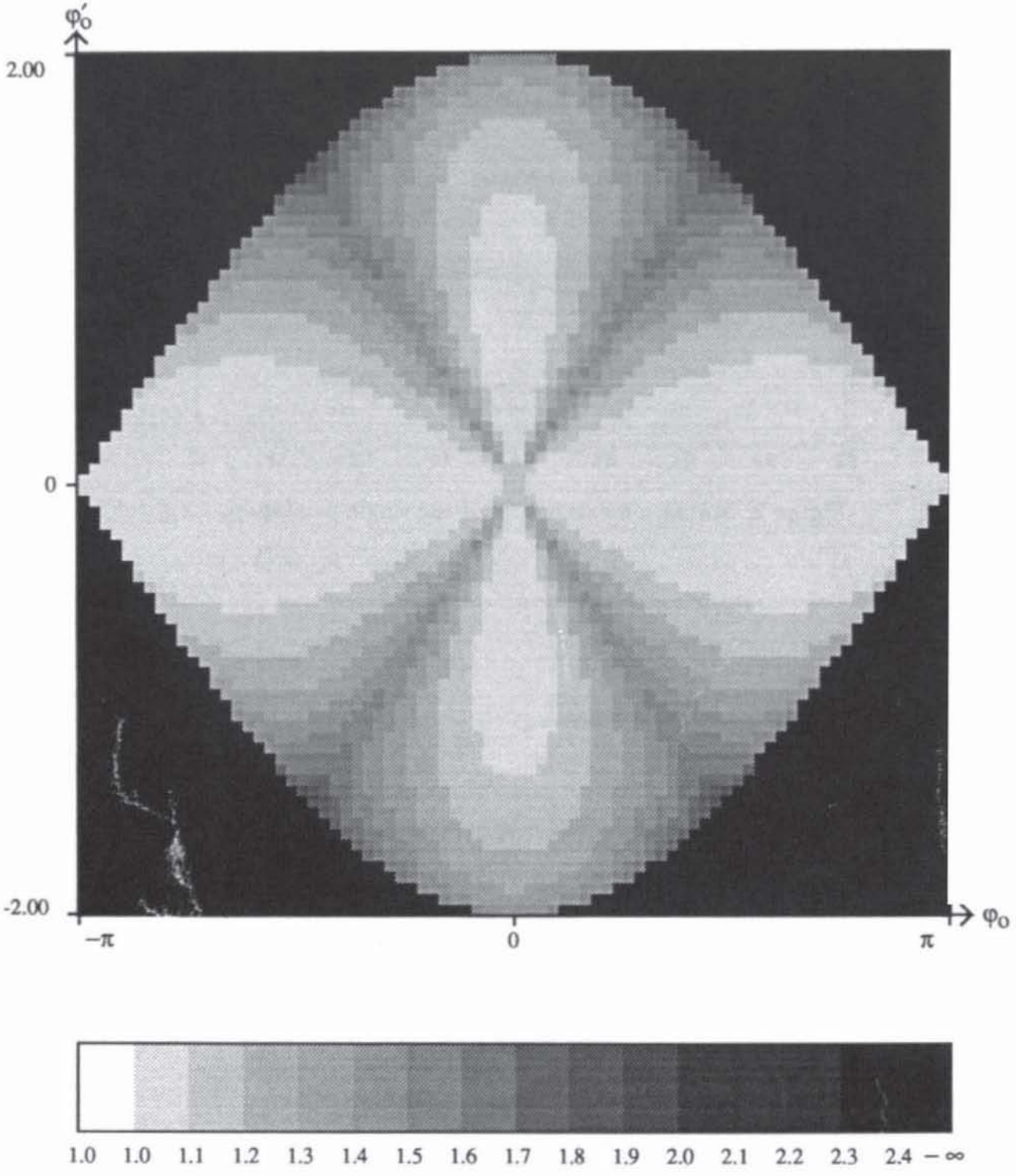

Figure 4: Stability measure $IS1_T$ of the single pendulum for $T = 100$.

The numerical analysis uses the state space representation of (51) which follows as

$$\begin{bmatrix} \varphi' \\ \varphi'' \end{bmatrix} = \begin{bmatrix} \varphi' \\ -\sin\varphi \end{bmatrix} . \tag{56}$$

The numerical simulation yields the same results as shown in Figure 2 to 4.

3.4 The double pendulum

The equations of the double pendulum in the standardized form result in

$$\begin{bmatrix} (1+\lambda_1)\lambda_2^2 & \lambda_2\cos(\alpha_1-\alpha_2) \\ \lambda_2\cos(\alpha_1-\alpha_2) & 1 \end{bmatrix} \begin{bmatrix} \alpha_1'' \\ \alpha_2'' \end{bmatrix} + \begin{bmatrix} \sin(\alpha_1-\alpha_2)\lambda_2^2\alpha_2'^2 \\ -\sin(\alpha_1-\alpha_2)\lambda_1^2\alpha_1'^2 \end{bmatrix} = \begin{bmatrix} (1+\lambda_1)\lambda_2\sin\alpha_1 \\ -\sin\alpha_2 \end{bmatrix} , \tag{57}$$

and may be rewritten in state space representation, too. Then, the state vector reads as $\mathbf{x} = [\alpha_1, \alpha_2, \alpha_1', \alpha_2']^T$. A thorough numerical analysis was performed by Hu [17]. For the graphical representation the software for cell mapping methods developed by Schaub [18] was extensively used.

The first step of the analysis requires the integration of the equations of motion. A typical result is shown in Figure 5. This information is used to evaluate the stability measure $IS1_T$ as a function of the time interval T considered, see Figure 6. Secondly, by variation of all initial conditions, the stability measure $IS2$ is obtained, Figure 7. A comparision between Figure 2 and Figure 7 shows that the double pendulum is much more sensitive to the initial disturbances in the displacement than the single pendulum.

It is interesting to analyze the double pendulum also for larger initial displacements, Figure 9. It turns out that there are two clearly separated regions. The left and right dark regions represent chaotic behaviour. There is a very high sensitivity to the initial conditions as Figure 8 shows. From this point of view, the boundary $||\mathbf{x}_0|| = 0.72$ in Figure 7 is due to chaotic behaviour and not to simple instability. But from an engineering point of view, both chaos and instability, are not acceptable.

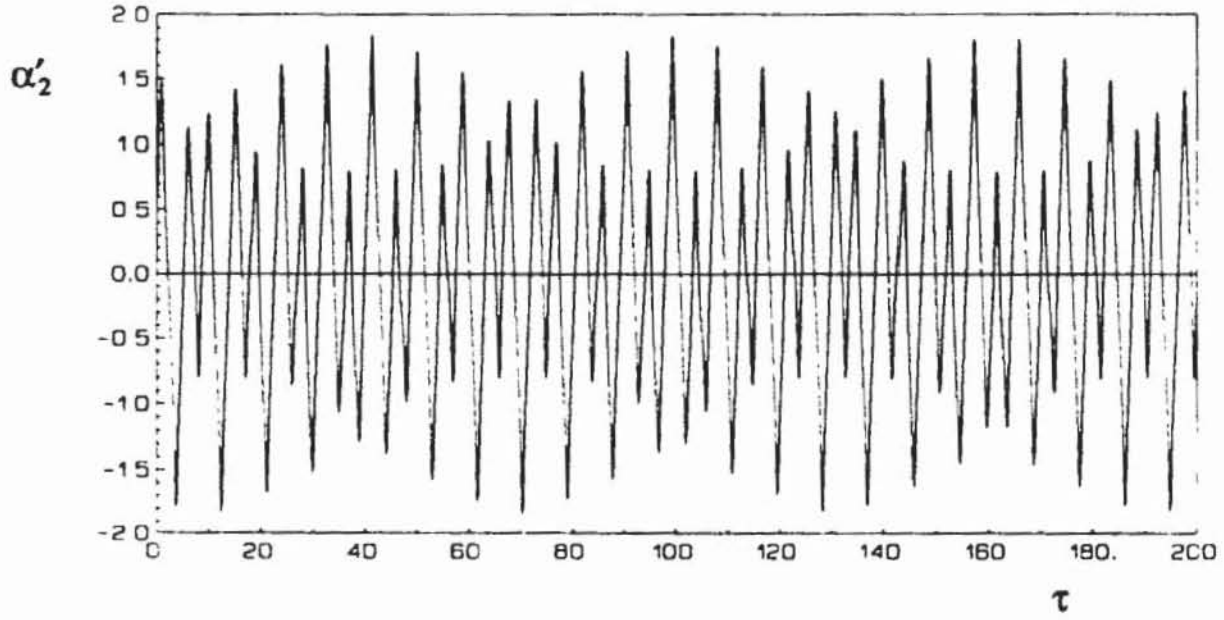

Figure 5: Trajectory α_2' of the double pendulum, $\lambda_1 = \lambda_2 = 1$ and $\alpha_{10} = 0,5$, $\alpha_{20} = -0,5$, $\alpha_{10}' = \alpha_{20}' = 0,5$.

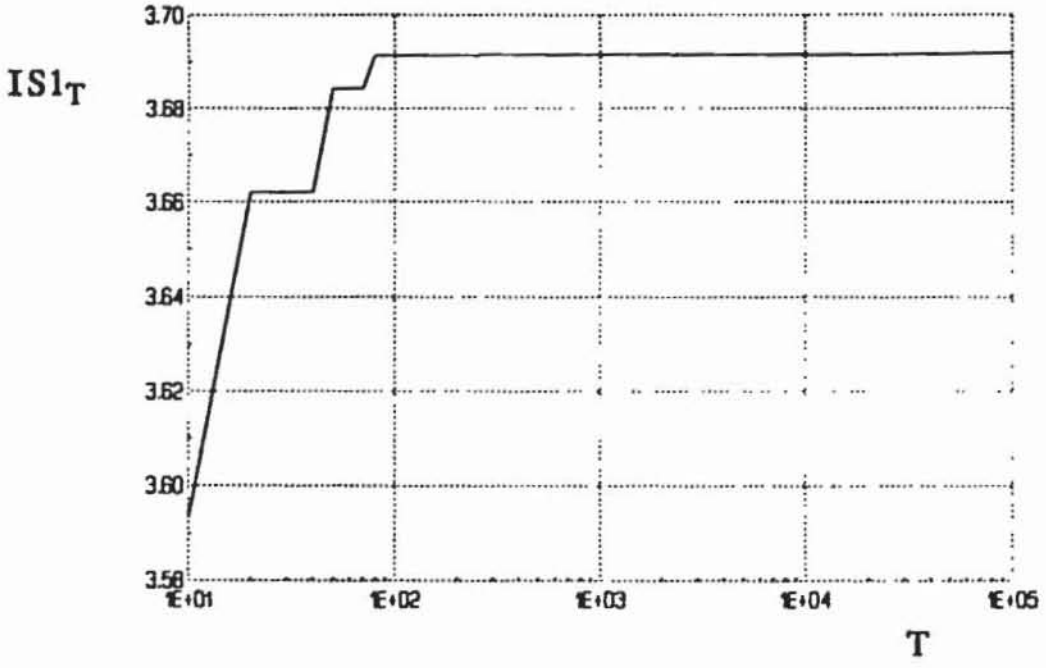

Figure 6: Stability measure $IS1_T$ as a function of T for the double pendulum, $\lambda_1 = \lambda_2 = 1$ and $\alpha_{10} = 0,5$, $\alpha_{20} = -0,5$, $\alpha_{10}' = \alpha_{20}' = 0,5$.

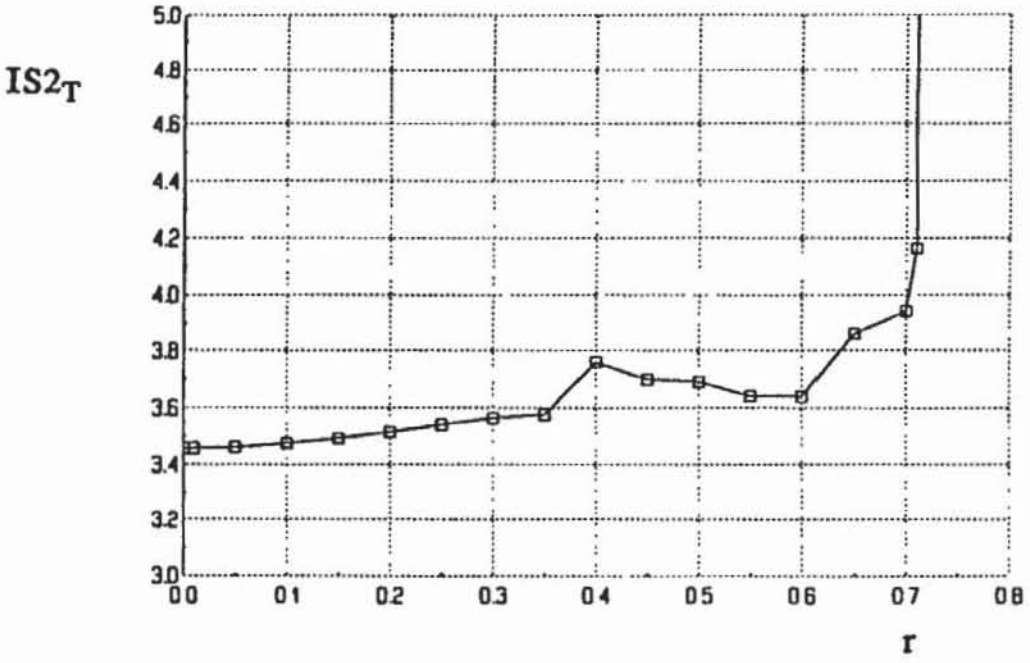

Figure 7: Stability measure $IS2$ of the double pendulum for $T = 100$.

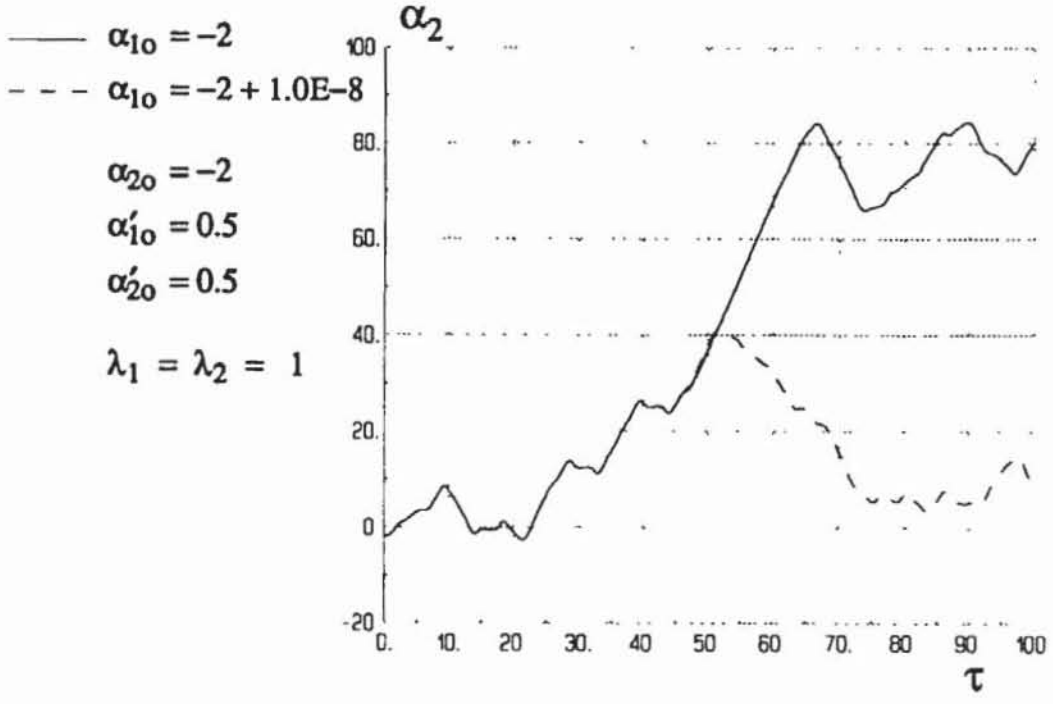

Figure 8: Sensitivity of the motion on the initial conditions.

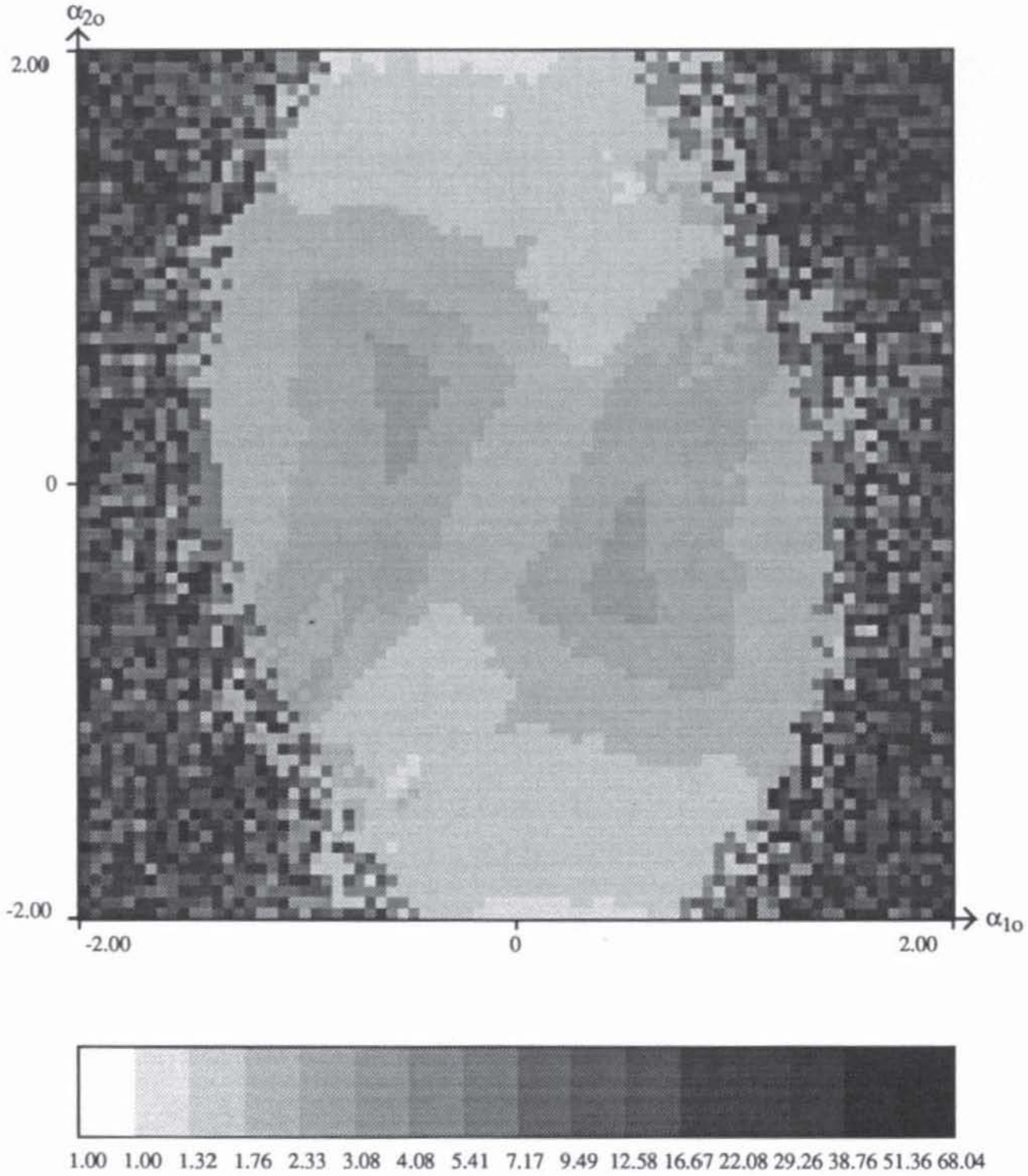

Figure 9: Stability measure $IS1_T$ of the double pendulum for $T = 100$, $\alpha'_{10} = \alpha'_{20} = 0,5$.

4 Conclusion

Multibody systems result in highly nonlinear equations of motion. For engineering applications only bounded motions are acceptable. The approach of stability measures allows the systematic computation of a basin of bounded motions for systems of arbitrary dimension. Then, the sensitivity of the systems to initial conditions and parameters can be investigated in more detail. The stability measures are not related to the frequency of the system response, they consider the absolute value of all state variables often important in the engineering design of mechanical systems.

References

[1] Wittenburg, J.: *Dynamics of Systems of Rigid Bodies.* Stuttgart: Teubner 1977.

[2] Schiehlen, W.: *Technische Dynamik.* Stuttgart: Teubner 1986.

[3] Roberson, R.E. and Schwertassek, R.: *Dynamics of Multibody Systems.* Berlin: Springer Verlag 1988.

[4] Nikravesh, P.E.: *Computer aided Analysis of Mechanical Systems.* New Jersey: Prentice Hall 1988.

[5] Haug, E.J.: *Computer-aided Kinematics and Dynamics of Mechanical Systems.* Boston: Allyn and Bacon 1989.

[6] Shabana, A.: *Dynamics of Multibody Systems.* New York: Wiley 1989.

[7] Magnus, K. (ed): *Dynamics of Multibody Systems.* Berlin: Springer-Verlag 1978.

[8] Slibar, A.; Springer, H. (eds): *Dynamics of Vehicles on Roads and Railway Tracks.* Swets and Zeitlinger 1978.

[9] Haug, E.J. (ed): *Computer-aided Analysis and Optimization of Mechanical System Dynamics.* Berlin: Springer-Verlag 1984.

[10] Kortüm, W.; Schiehlen, W.: General purpose vehicle system dynamics software based on multibody formalisms. *Vehicle System Dynamics* 14 (1985), 229-263.

[11] Bianchi, G.; Schiehlen, W. (eds): *Dynamics of Multibody Systems.* Berlin: Springer-Verlag 1986

[12] Kortüm, W.; Sharp, R.S.: A report on the state-of-affairs on "Application of Multibody Computer Codes to Vehicle System Dynamics". *Vehicle System Dynamics* 20 (1991), 177-184

[13] Schiehlen, W. (ed): *Multibody Systems Handbook* Berlin: Springer-Verlag 1990

[14] Otter, M.; Hocke, M; Daberkow, A.; Leister, G.: An object oriented data model for multibody systems. In: *Advanced Multibody System Dynamics*. Schiehlen, W. (ed). Dordrecht: Kluwer 1993, 19 48.

[15] Hahn, W.: *Stability of Motion*. Berlin: Springer Verlag 1967.

[16] Müller, P.C.: *Stabilität und Matrizen*. Berlin: Springer Verlag 1977.

[17] Hu, B.: *Stabilitätsmaß nichtlinearer Systeme*. Studienarbeit STUD 93. Stuttgart: Institut B für Mechanik 1992.

[18] Schaub, S.: *Interpolationsverfahren für Zellabbildungsmethoden*. Diplomarbeit DIPL-30. Stuttgart: Institut B für Mechanik 1990.